Surface migrations of endohedral Li^+ on the inner wall of C_{60}

V. Bernshtein and I. Oref*
Department of Chemistry, Technion-Israel Institute of Technology, Haifa 32000, Israel
(Received 28 February 2000; published 3 August 2000)

Quasiclassical trajectory calculations are used to study the dynamics of endohedral Li^+ ion migration along the inner wall of the C_{60} cage. The migration involves ion hopping (isomerization) from ring to ring via minimum-energy paths. The thermal rate coefficients for five- to six-member ring isomerization, k_5, and for six- to five- and six- to six-member ring isomerization, k_6, are given by the expressions $k_5=(4.0\times10^{14})\exp[(-7800\ \text{cal})/\text{RT}]\ \text{s}^{-1}$ and $k_6=(5.6\times10^{14})\exp[(-10\,000\ \text{cal})/\text{RT}]\ \text{s}^{-1}$. The present work establishes that the ion is not static but moves around along the walls of the molecular cage.

PACS number(s): 61.48.+c, 71.20.−b, 72.80.−r

I. INTRODUCTION

Gas-phase collisions between a rare-gas ion or an alkali-metal ion and a C_{60} molecule or between a C_{60} ion and bath-gas molecules can result in the formation of exohedral complexes where the ion resides on the outer surface of the fullerene molecule or in an endohedral complex $M^+@C_{60}$ with the ion inside the molecular cage [1–16]. The latter family of compounds, in addition to its obvious scientific interest, has technological significance as high-temperature superconductors and as important components in nanosize electronic and optical devices. *Ab initio* calculations have been performed [17–20] to determine the parameters of the potential-energy surface (PES) and the stability of the endohedral system. Ion/C_{60} intermolecular potentials have been developed [21–23] and used in molecular-dynamics simulations of experiments [17,21,24,25].

Quasiclassical trajectory calculations have been used [25] to study processes that occur in a high-energy collision of Li^+ with C_{60}. The degree of $Li@C_{60}^+$ formation as a function of the relative translational energy was determined, and the escape from the cage, following endohedral formation, was followed as a function of the relative translational energy. The collisional energy transfer probability density function $P(E',E)$ in inelastic collisions was determined and combined with the Rice-Ramsperger-Kassel-Marcus (RRKM) theory rate coefficient $k(E)$ to give the degree of dissociation of the excited C_{60}. In addition, the intramolecular energy redistribution following the initial impact of the Li^+ in the center of a pentagonal ring on the surface of the C_{60} was followed.

The multiple-well potential-energy surface of the system determines the location of the ion, which, in turn, determines the spectroscopy of the system [26,20,27,28]. Dunlap, Ballester, and Schmidt have calculated the PES for $M^+@C_{60}$ using all-electron local-density-functional total-energy calculations [20(a)]. For the case of the Li^+ ion they find that the minimum in the PES is at 0.14 nm from the center of the cage for the fivefold axis and at 0.12 nm for the threefold axis. The depth of the well relative to the center of the C_{60} is 0.51 eV for both structures. Endohedral vibrations are reported at ~350 cm^{-1}. The results of *ab initio* Hartree-Fock calculations by Varganov, Avramov, and Ovchinnikov [20(b)] also show that the Li^+ is located off center and that the minima in the PES are located in the centers of the pentagonal and hexagonal rings. Joslin *et al.* [27] have used the PES of Dunlap, Ballester, and Schmidt [20(a)] to calculate the vibrational-rotational bands of $Li^+@C_{60}$. They find a pure rotation peak near 40 cm^{-1} and a fundamental vibration-rotation band at 350 cm^{-1}. Hernandez-Rojas, Breton, and Gomez Llorente [29] have used a pairwise Lennard-Jones potential for the endohedral interaction and have calculated the rotational spectra of $M^+@C_{60}$.

There is also a dynamic aspect to the subject. The ion can be in motion, hopping from one adjacent well to another, each one located in the center of a ring, or moving almost freely inside the cage from one ring to the opposite ring. The dynamics of the system is obviously a function of the internal energy, which influences the physical characteristics of the system. It is the purpose of the present work to investigate the dynamics of endohedral Li^+ in C_{60} as a function of the internal energy of the system.

II. THEORY

Quasiclassical trajectory calculations were performed on $Li^+@C_{60}$ with a known PES and given initial conditions. The results were analyzed and rate coefficients for the Li^+ migration inside the cage wall were determined as a function of the temperature and the initial position of the ion. The details of the calculations are given below.

The numerical methods used in the present work are reported in Refs. [30,31]. The equations of motion were integrated by using a modified public domain program VENUS [32]. The intermolecular potential used is a carbon/ion pairwise potential [22,24]. It combines the repulsive part of a Lennard-Jones potential with an ion-atom attractive part whose $1/r^4$ dependence is derived from the Hellmann-Feynman theorem [24],

$$V_{\text{C-ion}}=4\epsilon[(\sigma_{\text{Ci}}/r)^{12}/z^2-(\sigma_{\text{Ci}}/r)^4], \tag{1}$$

where $\epsilon=78.4\,\text{meV}$ [23], $\sigma_{\text{Ci}}=(\sigma_{\text{C}^+}+\sigma_{\text{Li}^+})/2$, $\sigma_{\text{C}}=0.284\,\text{nm}$, $\sigma_{\text{Li}^+}=0.136\,\text{nm}$, and z is the ionic charge. This potential is in good agreement with *ab initio* calculations reported in Ref. [20].

*Electronic address: chroref@aluf.technion.ac.il

 ©2000 The American Physical Society

The intramolecular harmonic potential includes all the normal-mode contributions, stretching, bending, and nonbonded interactions between second-neighbor atoms [23]. A reasonable approximation is to apply one force constant for all the short C-C distances and one for the long C-C distances. The same approximation was used for the bending force constants. The values of the parameters of this potential were obtained from Procacci *et al.* [23]. The initial rotational energy was chosen from the appropriate thermal energy distributions. The internal energy was the average thermal energy of the endohedral complex at each temperature. Two initial configurations were chosen: the ion was placed at the center of either the five- or the six-member ring.

The ion migration on the surface was considered as an isomerization reaction for which the reaction occurred when the ion in the center of a five-member ring migrated to any of the five neighboring six-member rings ($5\rightarrow6$) or when the ion in the center of a six-member ring migrated to one of the three neighboring five-member rings ($6\rightarrow5$) or to one of the three neighboring six-member rings ($6\rightarrow6$). The reaction coordinate for each process was determined from Eq. (1) and it was verified that it is the minimum-potential energy path. The barriers are similar to those that were obtained by *ab initio* calculations [20]. The product of a reaction was defined by its final configuration. The distances between the ion and the carbon atoms surrounding it were calculated as a function of the trajectory time, and when the distances in the product configuration were shorter than those of the reactant, the reaction was declared over. The $5\rightarrow6$ isomerization is a unimolecular reaction with the rate coefficient k_5 given by

$$\frac{d\ln(N_{\mathrm{nr}}/N_{\mathrm{tot}})}{dt}=-k_5, \tag{2}$$

where N_{nr} is the number of nonreactive trajectories at time t and N_{tot} is the total number of trajectories. For the $6\rightarrow5$ and $6\rightarrow6$ cases, with rate coefficients k_{65} and k_{66}, respectively, the overall rate coefficient k_6 is also given by Eq. (2). The individual rate coefficients k_{65} and k_{66} are given by

$$N_r(j)=\frac{k_{6j}N_{\mathrm{tot}}}{k_6}[1-\exp(-k_6t)], \tag{3}$$

where j indicates a five- or a six-member ring. $N_r(j)$ indicates the number of reactive trajectories leading to ring j. The trajectory data were plotted as required by Eqs. (2) and (3) and the graphs were fitted by a linear least-squares fitting. The values of the rate coefficients were obtained from the slopes of the lines.

Quantum chemical calculations are the preferable method for studying the dynamics of chemical reactions. However, they are impractical for most systems, especially systems as complex as fullerenes. *Ab initio* molecular dynamics calculations have been used [20(c),20(d)] for $Li^+@C_{60}$ but the duration of the dynamic processes were limited to 75 fs, two orders of magnitude shorter than realistic reaction times in thermal systems of temperatures up to 900 K. Therefore, quasiclassical trajectory calculations are the method of choice. However, when quasiclassical trajectory calculations are used for studying chemical reactions there is the question of the flow of the zero-point energy (ZPE) from various vibrational modes of the molecule into the reaction coordinate [33,34]. Various methods have been suggested to correct for this deficiency. Analysis and comparison of some of the methods are given by Lim [35]. In one method the trajectories with product internal energy below the ZPE are replaced by new trajectories [36]. In another approach [37], a correction factor proportional to the transition-state sum of states is applied to the calculated rate coefficient of the reaction. Other correction methods are more complicated and involve adjusting the trajectories as the calculations progress [33,38–44,35]. In the present, endohedral, case there is surface diffusion, or ring hopping, of the Li^+ ion, which is akin to an isomerization reaction. The fact that the presence of Li^+ does not alter the normal-mode frequencies of the C_{60} is an indication that there are very weak Li^+-C interactions inside the C_{60} cage. Therefore, there is no question of leakage of ZPE from the C_{60} into the reaction coordinate, neither is there a question of the products of the isomerization having energy below the ZPE, because the energy release in the exit channel is greater than the ZPE of the Li^+-C_{60} modes.

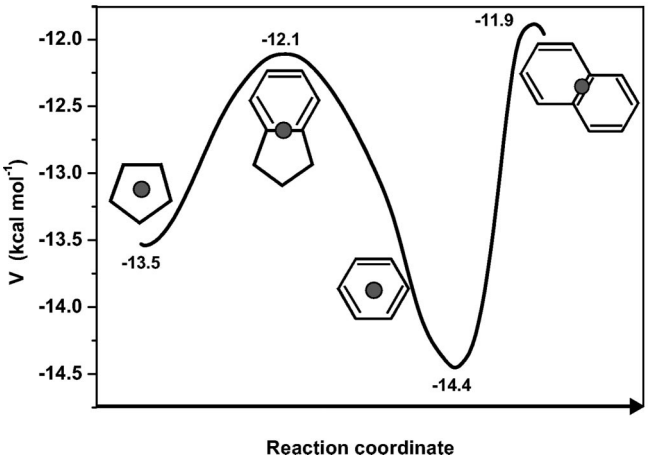

FIG. 1. The potential energy vs the reaction coordinate. The full circles indicate the positions of the ion above a ring at the bottom and top of the potential wells.

III. RESULTS AND DISCUSSION

As indicated before [20], the Li^+ inside the cage is at a potential-energy minimum located in the center of either a pentagonal or a hexagonal ring. Five hexagonal rings surround one pentagonal ring; therefore there exists only one fivefold-degenerate isomerization channel. Three pentagonal rings and three hexagonal rings, on the other hand, surround one hexagonal ring. This creates two parallel reaction channels. The reaction coordinate calculated from Eq. (1) is shown in Fig. 1. The activation energy for $5\rightarrow6$ is 1.4 kcal/mol, for $6\rightarrow5$ it is 2.3 kcal/mol, and for $6\rightarrow6$ it is 2.6 kcal/mol; the last two values are practically the same. The low values of the activation energies are due to the weak Li^+-C interactions and the fact that the ion experiences the

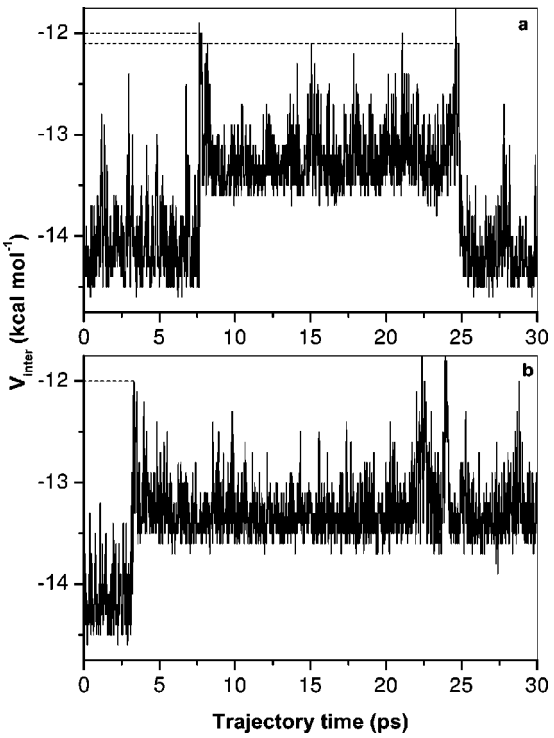

FIG. 2. The potential energy as a function of a trajectory time. (a) The trajectory describes the migration of an ion initially centered on a six-member ring to a five-member ring and then to a six-member ring. (b) A trajectory that describes the migration of an ion from a six- to a five-member ring.

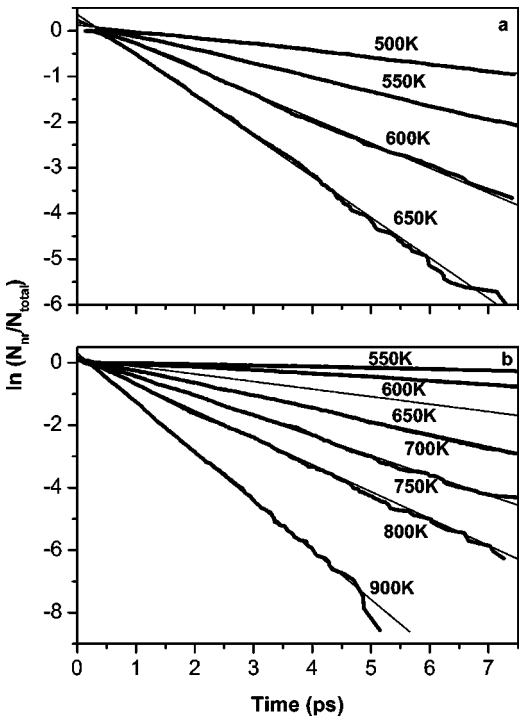

FIG. 3. (a) First-order plots of $5\rightarrow6$. (b) First-order plots of the combined $6\rightarrow5$ and $6\rightarrow6$ reactions. Heavy lines denote trajectory results and light lines are best fits to the data.

potential of non-nearest neighbors, which compensates for the potential energy lost during the movement of the ion along the reaction coordinate.

Sample trajectories are shown in Fig. 2, where the potential energy is shown as a function of time. Figure 2(a) shows an isomerization of $6\rightarrow5$ followed by an isomerization of $5\rightarrow6$. The ion is situated in the center of a hexagonal ring and it oscillates, gaining and losing energy to the C_{60} cage. When it acquires energy in the reaction coordinate above the value of the threshold energy for reaction, the ion migrates to the pentagonal ring, which has a higher potential energy. The spike height of -12 kcal/mol shows the instant when enough energy is obtained to cross the potential barrier of 2.3 kcal/mol. After spending ~17 ps above the pentagonal ring, isomerization occurs again and the ion migrates to one of the five neighboring hexagonal rings. The activation energy for this process is only 1.4 kcal/mol. Figure 2(b) shows a $6\rightarrow5$ isomerization, where the ion spends little time over a hexagonal ring before migrating to a pentagonal ring, where it stays for the rest of the trajectory. Trajectories for $6\rightarrow6$ isomerization are similar to the trajectories that are presented in Fig. 2 and are not shown here.

Trajectory calculations are subject to the availability of computational resources. That is to say, trajectories of long duration require prohibitive computational resources. Therefore, our computational approach was to run trajectories in a convenient temperature range, determine the Arrhenius parameters, and then extrapolate to values of the rate coefficients outside the computed range. The lower value of the temperature range of 500 K was determined by a time limit of 7.5 ps for a trajectory. Below this temperature, the degree of isomerization was too low for the results to be statistically meaningful. Above the upper limit of 900 K, the energy content of the system is very high and the ion is not following the minimum-energy path but rather flies from one side of the cage to the other instead of diffusing along the cage wall.

The rate coefficients for the Li^+ migration along the wall of the cage are found from plots of $\ln(N_{nr}/N_{tot})$ vs time [as in Eq. (2)], which are shown in Fig. 3 for $5\rightarrow6$ and the combined $6\rightarrow5$ and $6\rightarrow6$ isomerizations. The graphs are essentially linear and the values of k_5 and k_6 at each temperature are obtained from a linear fit to the data. In obtaining these graphs, care was taken that the number of trajectories was high enough so that the degree of conversion ranged from 25 % to 100 % in order to provide statistically meaningful results. The individual rate coefficients k_{65} and k_{66} are given by Eq. (3) and are calculated from the slopes of the graphs in Fig. 4. The linear least-squares fit was applied only to data with trajectory duration greater 0.3 ps. (Below this value, k is a function of time since at very short times there is more than one eigenvalue to the reaction velocity matrix [45]). The graphs are linear and therefore the rate coefficients obtained from them truly represent the individual isomerization reactions.

The predictive power of the present work is embedded in the Arrhenius equation $k=A\exp(-E_0/RT)$, where A is the frequency factor. The temperature range of this study was chosen to include an experimental study performed at 673 K by Campbell and co-workers [46]. Figure 5(a) shows the

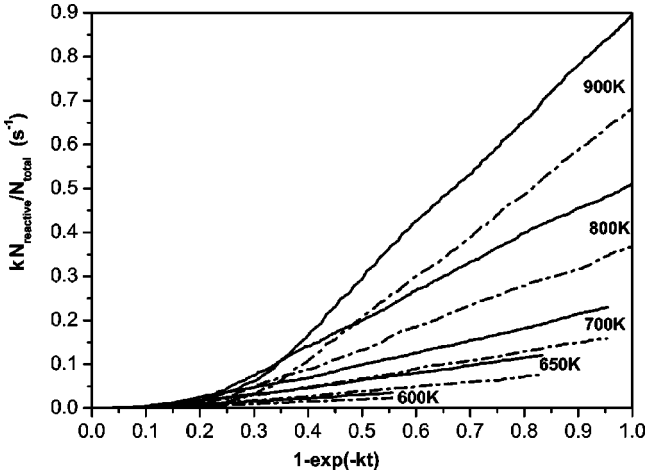

FIG. 4. A plot of the product of the total rate coefficients times the ratio of reactive to total trajectories for the $6\rightarrow5$ (——) and $6\rightarrow6$ (– – –) reactions. See text for details. The temperatures relate to the line above the value and to the line below it.

results for the $5\rightarrow6$ isomerization. The straight lines yield an A factor of $4.0\times10^{14}\,\mathrm{s}^{-1}$ and an activation energy of 7.8 kcal/mol. This is larger by a factor of more than 5 than the barrier height for this reaction. Figure 5(b) shows Arrhenius plots for reaction $6\rightarrow5$ and reaction $6\rightarrow6$ and for the combined rate coefficient of the two channels. The plots are not as linear as the plot in Fig. 5(a) but clearly an Arrhenius-type behavior is observed. When the data in Fig. 5(b) are limited

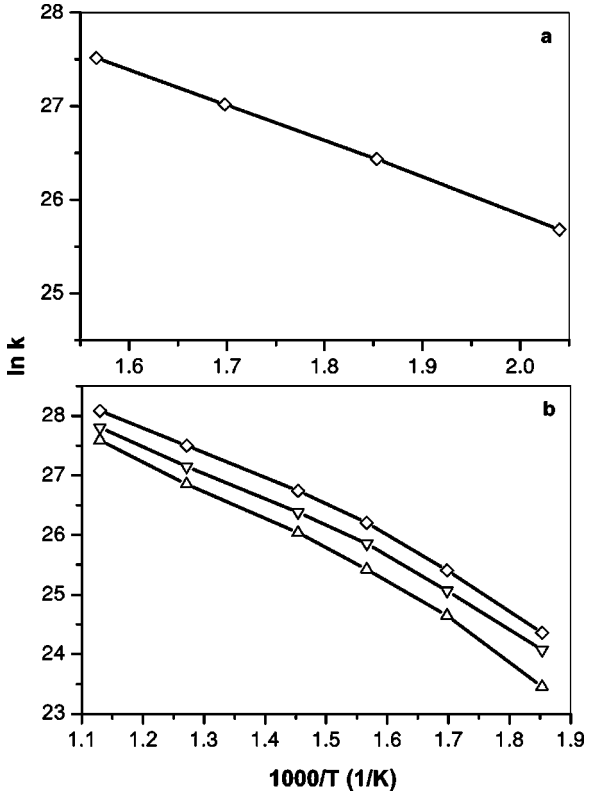

FIG. 5. Arrhenius plots for (a) $5\rightarrow6$ and (b) $6\rightarrow5$ (▽), $6\rightarrow6$ (△), and the overall k (◇).

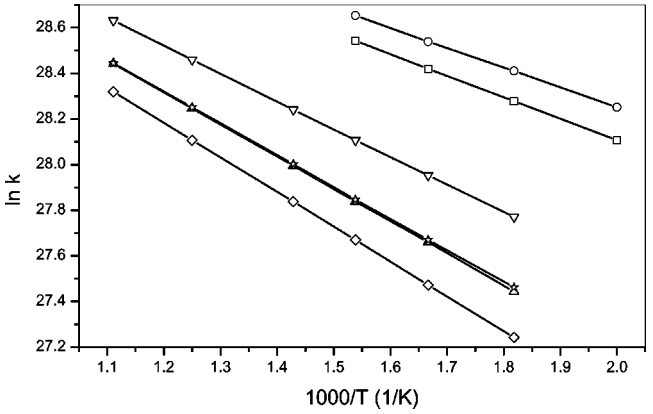

FIG. 6. Arrhenius plots of activated complex theory rate coefficients $5\rightarrow6$ (□), $6\rightarrow5$ (△), $6\rightarrow6$ (◇), and for RRKM theory rate coefficients, $5\rightarrow6$ (○), $6\rightarrow5$ (▽), $6\rightarrow6$ (☆).

to the same range as in Fig. 5(a), the graphs appear linear as well. A linear best fit to the data of the combined $6\rightarrow5$ and $6\rightarrow6$ reactions yields values of the Arrhenius parameters of $A=5.6\times10^{14}\,\mathrm{s}^{-1}$ and activation energy 10 kcal/mol.

Analysis of many trajectories indicates that, in the temperature range that was studied, the ion does not migrate through the center of the cage. Rather, it hops from one ring to the other along the inner wall of the cage. This is so because the highest barrier for migration along the wall is 2.6 kcal/mol for the $6\rightarrow6$ isomerization while the barrier for penetration through the center is 10.3 kcal/mol. Therefore, the ion follows the lowest-energy path along the wall and avoids jumping from one ring to another through the center.

We have applied the activated complex theory (ACT) and the Rice-Ramsperger-Kassel-Marcus theory to the $Li^+@C_{60}$ system in order to calculate the rate coefficients for $5\rightarrow6$, $6\rightarrow5$, and $6\rightarrow6$ isomerization. The results are presented in Fig. 6. Both calculations yield similar results with values of k_{ACT} smaller by 10–13 % from values of k_{RRKM}. They are different, however, from the trajectory results shown in Fig. 5. A comparison of the values of k_{ACT} and k_{RRKM} with k_{traj} shows that the trajectory results yield activation energies that are about fourfold larger than the values obtained by the conventional ACT and RRKM methods. However, the A factors of k_{traj} are much larger than the A factors of k_{ACT} and of k_{RRKM}, making the difference in values of the rate coefficients much smaller. At 550 K, the difference is a factor of ~2 and at 900 K the difference is only a few percent. Generally speaking, however, the ACT or the RRKM theory cannot simulate the trajectory results very well.

Since k_{ACT} is expected to exhibit Arrhenius-type behavior, the straight lines in Fig. 6 are no surprise. However, the Arrhenius-type behavior of the RRMK theory rate coefficients $k(E)$ is somewhat of a surprise, since they are obtained from an expression with no obvious exponential behavior,

$$k(E)=\frac{W(E^+)}{h\rho(E)}, \tag{4}$$

where $W(E^+)$ indicates the number of states of the complex, E^+ is the internal energy of the complex, and $\rho(E)$ is the density of states of the endohedral complex. The Arrhenius-type behavior of $k(E)$ has been noted before for microcanonical systems where the internal energy was converted to a vibrational temperature, which served as the independent parameter of the Arrhenius equation [47,48]. In the present case, the values of $k(E)$ are calculated at the average energies of the canonical ensemble and the temperature is the ensemble temperature, which is the inverse of the previous case.

The exohedral complex represents a totally different situation from the endohedral case, which is discussed here, because, in addition to isomerization, there is dissociation where the ion leaves the C_{60} molecule completely. The potential surface is different and the barriers for isomerization/dissociation are much higher, which makes the dissociation much slower and the demand on the computational facilities higher. Work on the exohedral case is in progress and will be reported separately.

In conclusion, quasiclassical trajectory calculations are used to study the Li^+ ion migration along the inner wall of a C_{60} molecule. Starting from initial conditions where the ion is located in the center of a five- or six-member ring, the migration of the ion is computed. A statistically significant number of trajectories are used to evaluate rate coefficients as function of the temperature. A plot of the logarithm of the rate coefficients vs $1/T$ is linear for five- to six-member ring isomerization and nearly linear for six- to five- or six- to six-member rings. The Arrhenius parameters that are reported enable the calculations of ion migration at experimental temperatures. The present work establishes the fact that the Li^+ ion is not static but moves around the C_{60} cage.

ACKNOWLEDGMENTS

This work is supported by the Technion V. P. R. Fund, by the B. and N. Ginsburg Energy Research Fund, and by the Ministry of Science and the Arts.

[1] M. Saunders, H. A. Jimenez-Vasques, R. J. Cross, and R. J. Poreda, Science **259**, 1428 (1993).
[2] M. Saunders, H. A. Jimenez-Vasques, R. J. Cross, S. Mroczkowski, M. Cross, D. E. Giblin, and R. J. Poreda, J. Am. Chem. Soc. **116**, 2193 (1994).
[3] M. Saunders, R. J. Cross, H. A. Jimenez-Vasques, R. Shimshi, and A. Khong, Science **271**, 1693 (1996).
[4] Z. Wan, J. F. Christian, and S. L. Anderson, J. Chem. Phys. **96**, 3344 (1992).
[5] J. F. Christian, Z. Wan, and S. L. Anderson, J. Chem. Phys. **99**, 3468 (1993).
[6] Y. Basir and S. L. Anderson, J. Chem. Phys. **107**, 8370 (1997).
[7] Z. Wan, J. F. Christian, and S. L. Anderson, Phys. Rev. Lett. **69**, 1352 (1992).
[8] Z. Wan, J. F. Christian, Y. Basir, and S. L. Anderson, J. Chem. Phys. **99**, 5858 (1993).
[9] T. Weiske, D. K. Bohme, J. Hrusak, W. Kratschmer, and H. Schwarz, Angew. Chem. **103**, 989 (1991).
[10] T. Weiske, D. K. Bohme, J. Hrusak, W. Kratschmer, and H. Schwarz, Angew. Chem. Int. Ed. Engl. **30**, 884 (1991).
[11] M. M. Ross and J. H. Callahan, J. Phys. Chem. **95**, 5720 (1991).
[12] T. Wong, J. K. Terlouw, T. Weiske, and H. Schwarz, Int. J. Mass Spectrom. Ion Processes **113**, 23 (1992).
[13] R. C. Mowrey, M. Ross, and J. H. Callahan, J. Phys. Chem. **96**, 4755 (1992).
[14] R. Shimshi, R. J. Cross, and M. Saunders, J. Am. Chem. Soc. **119**, 1163 (1997).
[15] R. Tellgmann, N. Krawez, S. H. Lin, I. V. Hertel, and E. E. B. Campbell, Nature (London) **382**, 407 (1996).
[16] E. E. B. Campbell, R. Tellgmann, N. Krawez, and I. V. Hertel, J. Phys. Chem. Solids **58**, 1763 (1997).
[17] R. C. Mowrey, M. Ross, and J. H. Callahan, J. Phys. Chem. **96**, 4755 (1992).
[18] L. Pang and F. Brisse, J. Phys. Chem. **97**, 8562 (1993).
[19] S. Patchkovskii and W. Thiel, J. Chem. Phys. **106**, 1796 (1997).
[20] (a) B. I. Dunlap, J. L. Ballester, and P. P. Schmidt, J. Phys. Chem. **96**, 9781 (1992); (b) S. A. Varganov, P. V. Avramov, and S. G. Ovchinnikov, Fiz. Tverd. Tela (St. Petersburg) **42**, 378 (2000) [Phys. Solid State **42**, 388 (2000)]; (c) K. Ohno, Y. Maruyama, K. Esfarjani, Y. Kawazoe, N. Sato, R. Hatakeyama, T. Hirata, and M. Niwano, Phys. Rev. Lett. **76**, 3590 (1996); (d) A. A. Farajian, K. Onho, K. Esfarjani, Y. Maruyama, and Y. Kawazoe, J. Chem. Phys. **111**, 2164 (1999).
[21] D. W. Brenner, Phys. Rev. B **42**, 9458 (1990).
[22] J. Breton, J. Gonzales-Platas, and C. Girardet, J. Chem. Phys. **99**, 4036 (1993).
[23] P. Procacci, G. Cardini, P. Salvi, and V. Schettino, Chem. Phys. Lett. **195**, 347 (1992).
[24] T. Kaplan, M. Rasolt, M. Karimi, and M. Mostoller, J. Phys. Chem. **97**, 6124 (1993).
[25] V. Bernstein and I. Oref, J. Chem. Phys. **109**, 9811 (1998); Chem. Phys. Lett. **313**, 52 (1999).
[26] J. L. Ballester and B. I. Dunlap, Phys. Rev. A **45**, 7985 (1992).
[27] C. G. Joslin, J. Yang, C. G. Grey, S. Goldman, and J. D. Poll, Chem. Phys. Lett. **208**, 86 (1993).
[28] C. G. Joslin, C. G. Grey, S. Goldman, J. Yang, and J. D. Poll, Chem. Phys. Lett. **215**, 144 (1993).
[29] J. Hernandez-Rojas, J. Breton, and J. M. Gomez Llorente, J. Chem. Phys. **104**, 1179 (1996).
[30] V. Bernshtein, K. F. Lim, and I. Oref, J. Phys. Chem. **99**, 4531 (1995).
[31] D. C. Clary, R. G. Gilbert, V. Bernshtein, and I. Oref, Faraday Discuss. **102**, 423 (1995).
[32] W. L. Hase, R. J. Duchovic, X. Hu, A. Komornicki, K. F. Lim, D.-H. Lu, G. H. Peslherbe, K. N. Swamy, S. R. Vande-Linde, A. Varandas, H. Wang, and R. J. Rolf, Quantum Chem. Prog. Exch. Bull. **16**, 43 (1996) (QCPE program 671).
[33] J. M. Bowman, B. Gazdy, and Q. Sun, J. Chem. Phys. **91**, 2859 (1989).

[34] W. H. Miller, W. L. Hase, and C. L. Darling, J. Chem. Phys. **91**, 2863 (1989).
[35] K. F. Lim, J. Chem. Soc., Faraday Trans. **93**, 669 (1997).
[36] A. J. Varandas and J. M. C. Marques, J. Chem. Phys. **100**, 1908 (1994).
[37] D. L. Shen and H. O. Pritchard, J. Chem. Soc., Faraday Trans. **92**, 4357 (1996).
[38] G. H. Peslherbe and W. L. Hase, J. Chem. Phys. **100**, 1179 (1994).
[39] M. Ben-Nun and R. D. Levine, J. Chem. Phys. **101**, 8768 (1994).
[40] K. F. Lim and D. A. McCormack, J. Chem. Phys. **102**, 1705 (1995).
[41] D. A. McCormack and K. F. Lim, J. Chem. Phys. **103**, 1995 (1991).
[42] D. A. McCormack and K. F. Lim, J. Chem. Phys. **107**, 572 (1997).
[43] D. A. McCormack and K. F. Lim, Phys. Chem. Chem. Phys. **1**, 1 (1999).
[44] G. Stock and U. Moeller, J. Chem. Phys. **111**, 65 (1999); **111**, 77 (1999).
[45] V. Bernshtein and I. Oref, J. Phys. Chem. **97**, 6830 (1993).
[46] E. E. B. Campbell (private communication).
[47] I. Oref and N. Gordon, J. Phys. Chem. **82**, 2035 (1978).
[48] J. Park, R. Bersohn, and I. Oref, J. Chem. Phys. **93**, 5700 (1990).